Pyroxenite melting at subduction zones

Bowman and Ducea, Supplemental Material

DATA FILTERING METHODS

Only unaltered samples with Zn data as well as whole-rock major element oxide sums between 97 and 101 wt.% were included in the global geochemical database. To consider only primitive magmas, we removed samples with MgO contents less than 7 wt.% – to avoid magmas that have experienced significant cotectic crystallization – and greater than 17 wt.% – to filter out melts that have accumulated olivine (Le Roux et al., 2010). Reported major element oxide contents were then renormalized to a dry sum of 100 wt.%. Finally, to eliminate samples with anomalously alkalic geochemistry that are not representative of arc magmas, we discarded compositions which at a given SiO_2 content have total alkali contents ($Na_2O + K_2O$) that are more than 1.5 wt.% greater than the subalkaline limit (Luffi and Ducea, 2022).

CRUSTAL THICKNESS CALCULATIONS

Elevations of each sample were extracted from the National Oceanographic and Atmospheric Administration 1 arc-minute ETOPO1 global relief model (https://www.ngdc.noaa.gov/mgg/global/relief/ETOPO1). For each sample, we calculated Moho depth according to the Moho depth-elevation correlation of Luffi and Ducea (2022). Elevations and Moho depths were then summed together to determine the crustal thickness for each sample. We disregard the thickness of the lithospheric mantle, which is <20 km thick at most active arcs (e.g., Tassara et al., 2006; Till et al., 2013).

SPATIAL AVERAGING METHODS AND ERROR CALCULATIONS

To minimize sampling bias in our dataset such that each volcanic field is equally represented, we divided the spatial coverage of our compilation into 10 km x 10 km x 650 m (*L* x *W* x *h = 10 km x 10 km x 650 m)* prisms and calculated the median geochemical composition and crustal thickness for each volume unit. 1-sigma standard deviations were calculated for all averages. Due to the scarcity of primitive basalts in thick-crusted arcs, many prisms contain a single sample. In this case, the geochemical composition and crustal thickness associated with this single sample is taken as the 'median' for the corresponding prism. Uncertainties on values in the single-point prism dataset were taken as the median standard deviation of the corresponding values from the multi-point prism dataset. Crustal thickness data were also assigned a 1-sigma calibration error of ±2.5 km according to the error envelope on the Moho-depth-elevation correlation of Luffi and Ducea (2022). All errors on crustal thicknesses are thus root mean square errors that combine the calibration error with the uncertainty associated with spatially averaging the compilation.

When the spatially averaged geochemical dataset is further averaged, such as in Figure 2B, we report root mean square errors. To do this, in the case of SiO_2 for example, we calculate the median standard deviation on SiO_2 content and take this as the calibration error. We then calculate the median SiO_2 content and take the 1-sigma standard deviation of the median. Root mean square errors are then calculated for the median SiO_2 content by combining the calibration error with the standard deviation of the median.

REFERENCES CITED

Le Roux, V., Lee, C.-T.A., and Turner, S.J., 2010, Zn/Fe systematics in mafic and ultramafic
        systems: Implications for detecting major element heterogeneities in the Earth's mantle:

Geochimica et Cosmochimica Acta, v. 74, p. 2779–2796,

doi:https://doi.org/10.1016/j.gca.2010.02.004.

Luffi, P., and Ducea, M.N., 2022, Chemical mohometry: assessing crustal thickness of ancient

orogens using geochemical and isotopic data: Reviews of Geophysics, v. 60,

e2021RG000753, https://doi.org/10.1029/2021RG000753.

Ryan, W.B.F. et al., 2009, Global Multi-Resolution Topography synthesis: Geochemistry,

Geophysics, Geosystems, v. 10, doi:https://doi.org/10.1029/2008GC002332.

Tassara, A., Götze, H.-J., Schmidt, S., and Hackney, R., 2006, Three-dimensional density model

of the Nazca plate and the Andean continental margin: Journal of Geophysical Research:

Solid Earth, v. 111, doi:https://doi.org/10.1029/2005JB003976.

Till, C.B., Grove, T.L., Carlson, R.W., Donnelly-Nolan, J.M., Fouch, M.J., Wagner, L.S., and

Hart, W.K., 2013, Depths and temperatures of <10.5 Ma mantle melting and the

lithosphere-asthenosphere boundary below southern Oregon and northern California:

Geochemistry, Geophysics, Geosystems, v. 14, p. 864–879,
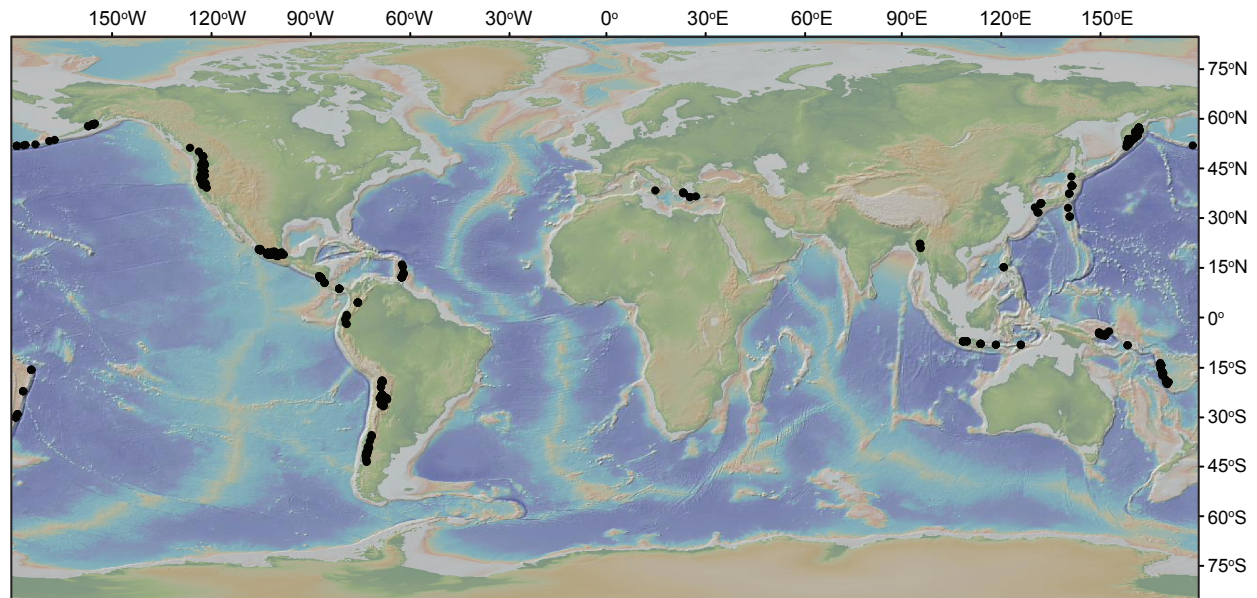
doi:https://doi.org/10.1002/ggge.20070.

Figure S1. Topographic map of the Earth (Global Multi-Resolution Topography Synthesis; Ryan et al., 2009) showing locations of samples (n=900) used to create a global database of Pliocene-Holocene primitive arc magmas.
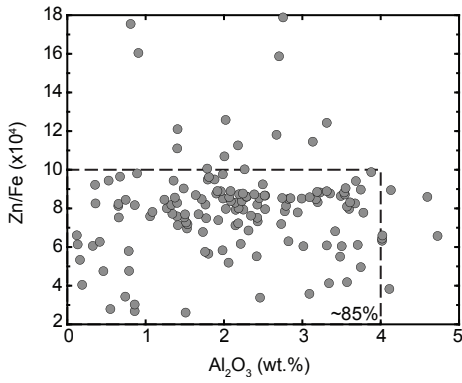
Zn/Fe (x10⁴)

18
16
14
12
10
8
6
4
2

0   1   2   3   4   5

~85%

Al₂O₃ (wt.%)

Figure S2. Zn/Fe ($\times 10^4$) vs. Al$_2$O$_3$ (wt.%) of sub-arc peridotites compiled from the GEOROC database. Only unaltered samples with Mg# = 88-91 and major element sums between 97 and 101 wt.% are included. The dash-lined box contains the ~85% of sub-arc peridotites that are not very fertile (Al$_2$O$_3$ <4 wt.%), have Zn/Fe ($\times 10^4$) <10, and are therefore unlikely to produce high (>12)-Zn/Fe melts.
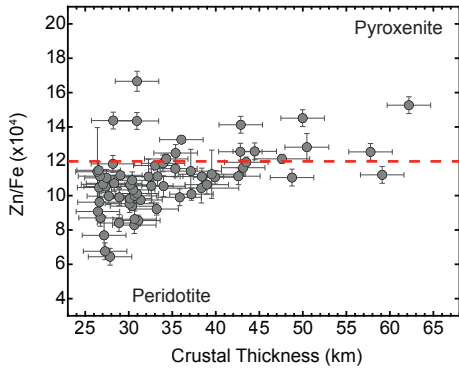
Figure S3. Median Zn/Fe ratios versus crustal thickness for all samples with median MgO >10 wt.%. Despite a lack of samples from the thickest-crusted arcs, the trend of increasing Zn/Fe with crustal thickness is apparent. Errors on Zn/Fe (x10^4) are 1-sigma standard deviations. Errors on crustal thickness are root mean square errors. The red dashed line delineates the fields of peridotite (Zn/Fe (x10^4) <12) and pyroxenite (Zn/Fe (x10^4) >12) melts.
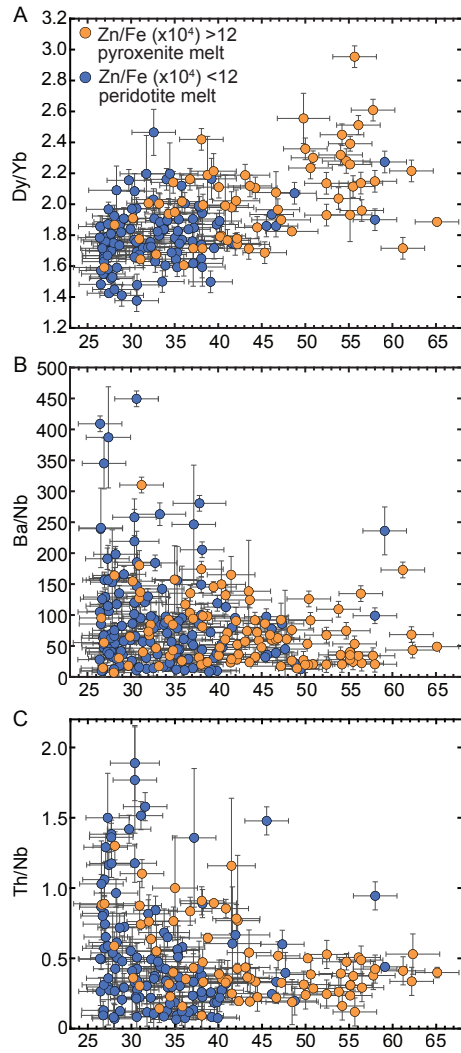
Figure S4. Median Dy/Yb (A), Ba/Nb (B), and Th/Nb (C) plotted against median crustal thickness. Samples are colored according to Zn/Fe ratios, where orange samples have Zn/Fe $(x10^4)$ >12 and are proposed to derive from pyroxenite. Blue samples have Zn/Fe $(x10^4)$ <12 and are interpreted to represent peridotite melts. Median Dy/Yb (A) increases with crustal thickness, consistent with garnet-present melting. Ba/Nb (B) is a sensitive proxy for the involvement of slab fluids, while Th/Nb (C) is a tracer of slab melts. Because peridotite- and pyroxenite-derived magmas have overlapping Ba/Nb and Th/Nb signatures, the slab does not play a significant role in differentiating the two suites of magmas. 1-sigma errors are shown for trace element ratios. Errors on crustal thicknesses are root mean square errors.
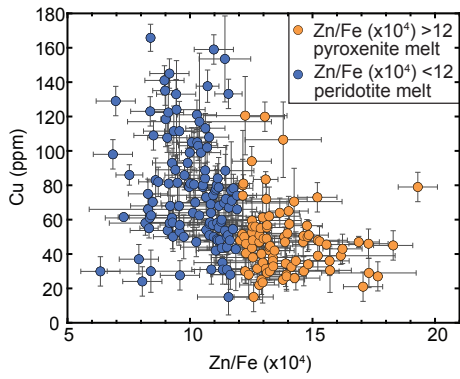
Figure S5. Median Cu content (ppm) plotted against median Zn/Fe ($\times 10^4$). Cu contents decrease with increasing Zn/Fe, indicating that pyroxenite melts (Zn/Fe $\times 10^4$ >12, orange points) are more depleted in copper compared to peridotite-derived magmas (Zn/Fe $\times 10^4$ <12, blue points). Error bars are 1-sigma standard deviations.